Nutrition Research and Practice

Original Research

Check for updates

Gynostemma pentaphyllum extract and Gypenoside L enhance skeletal muscle differentiation and mitochondrial metabolism by activating the PGC-1α pathway in C2C12 myotubes

Yoon Hee Kim [1], Jae In Jung [2], Young Eun Jeon [2], So Mi Kim [2], Tae Kyu Oh [1], Jaesun Lee [1], Joo Myung Moon [1], Tae Young Kim [1], and Eun Ji Kim [2§]

[1]Technology Development Center, BTC Corporation, Ansan 15588, Korea
[2]Regional Strategic Industry Innovation Center, Hallym University, Chuncheon 24252, Korea

OPEN ACCESS

§**Corresponding Author:**

Eun Ji Kim

Regional Strategic Industry Innovation
Center, Hallym University, 1 Hallymdaehak-gil,
Chuncheon 24252, Korea.
Tel. +82-33-248-3106
Fax. +82-33-244-3107
Email. myej4@hallym.ac.kr

ORCID iDs
Yoon Hee Kim
https://orcid.org/0000-0002-6045-9927
Jae In Jung
https://orcid.org/0000-0002-4475-1434
Young Eun Jeon
https://orcid.org/0000-0002-7312-8545
So Mi Kim
https://orcid.org/0000-0002-0174-3485
Tae Kyu Oh
https://orcid.org/0000-0002-2248-9017
Jaesun Lee
https://orcid.org/0000-0001-6857-4092

ABSTRACT

BACKGROUND/OBJECTIVES: Peroxisome proliferator-activated receptor-gamma co-activator-1α (PGC-1α) has a central role in regulating muscle differentiation and mitochondrial metabolism. PGC-1α stimulates muscle growth and muscle fiber remodeling, concomitantly regulating lactate and lipid metabolism and promoting oxidative metabolism. *Gynostemma pentaphyllum* (Thumb.) has been widely employed as a traditional herbal medicine and possesses antioxidant, anti-obesity, anti-inflammatory, hypolipemic, hypoglycemic, and anticancer properties. We investigated whether *G. pentaphyllum* extract (GPE) and its active compound, gypenoside L (GL), affect muscle differentiation and mitochondrial metabolism via activation of the PGC-1α pathway in murine C2C12 myoblast cells.

MATERIALS/METHODS: C2C12 cells were treated with GPE and GL, and quantitative reverse transcription polymerase chain reaction and western blot were used to analyze the mRNA and protein expression levels. Myh1 was determined using immunocytochemistry. Mitochondrial reactive oxygen species generation was measured using the 2′7′-dichlorofluorescein diacetate assay.

RESULTS: GPE and GL promoted the differentiation of myoblasts into myotubes and elevated mRNA and protein expression levels of Myh1 (type IIx). GPE and GL also significantly increased the mRNA expression levels of the PGC-1α gene (*Ppargc1a*), lactate metabolism-regulatory genes (*Esrra* and *Mct1*), adipocyte-browning gene fibronectin type III domain-containing 5 gene (*Fndc5*), glycogen synthase gene (*Gys*), and lipid metabolism gene carnitine palmitoyltransferase 1b gene (*Cpt1b*). Moreover, GPE and GL induced the phosphorylation of AMP-activated protein kinase, p38, sirtuin1, and deacetylated PGC-1α. We also observed that treatment with GPE and GL significantly stimulated the expression of genes associated with the anti-oxidative stress response, such as *Ucp2, Ucp3, Nrf2,* and *Sod2*.

CONCLUSIONS: The results indicated that GPE and GL enhance exercise performance by promoting myotube differentiation and mitochondrial metabolism through the upregulation of PGC-1α in C2C12 skeletal muscle.

Keywords: Gynostemma pentaphyllum; peroxisome proliferator-activated receptor gamma coactivator 1-alpha; muscle, skeletal

Generated by xmlinkpress

Joo Myung Moon (iD)
https://orcid.org/0000-0002-5750-9620
Tae Young Kim (iD)
https://orcid.org/0000-0003-1428-1176
Eun Ji Kim (iD)
https://orcid.org/0000-0001-9305-4769

Conflict of Interest
The authors declare no potential conflicts of interests.

Author Contributions
Conceptualization: Kim YH, Moon JM, Kim TY; Data analysis: Jung JI, Jeon YE, Kim SM, Kim EJ; Formal analysis: Jung JI, Jeon YE, Kim SM; Visualization: Kim YH, Oh TK, Lee J; Writing - original draft: Kim YH, Kim EJ; Writing - review & editing: Kim YH, Kim EJ.

INTRODUCTION

Skeletal muscles have key roles in supporting carbohydrate metabolism and energy expenditure as they contain numerous mitochondria [1-3]. Mitochondria are entirely responsible for increasing endurance-exercise tolerance of skeletal muscles to fatigue and improving energy metabolism, resulting in enhanced exercise performance [4]. This process generates cellular energy in the form of ATP production, intracellular calcium homeostasis, amino acid metabolism, oxidant–antioxidant balance, and apoptosis [5]. Skeletal muscle consists of 4 major myosin heavy chain (MyHC) fibers depending on the expression of slow-twitch with Myh7 (type I), fast-twitch with Myh2 (type IIa), Myh1 (type IIx), or Myh4 (type IIb) [6]. Myh7 fibers (slow-twitch, oxidative) are rich in mitochondria, resistant to fatigue, and sustain long-term energy demands. In addition, they facilitate fatty acid oxidation and more efficient ATP production. In contrast, Myh4 fibers (fast-twitch) contain glycogen and glucose as energy sources. These mitochondria-poor fibers primarily rely on rapid glycolysis for ATP production; thus, they are more sensitive to fatigue, which is attributed to sudden activity in a short duration [7]. Other fiber types such as Myh2 (fast-twitch, oxidative) and Myh1 (fast-twitch, oxido-glycolytic) show a combination of characteristics intermediate between those of Myh7 and Myh4 fibers [8-10].

Mitochondria undergo continuous biogenesis, generally via expression of *Ppargc1a*, the gene that encodes peroxisome proliferator-activated receptor-gamma coactivator 1α (PGC-1α) [11]. *Ppargc1a* overexpression in mice has been reported to enhance mitochondrial concentrations, exercise capacity, oxidative capacity, and fatigue resistance [12]. PGC-1α is a co-activator of a broad range of nuclear transcription factors, including nuclear respiratory factor (NRF) 1 and 2, estrogen-related receptor α (ERRα), as well as myocyte enhancer factor-2 (MEF-2). PGC-1α drives mitochondrial biogenesis via the expression of the gene that encodes mitochondrial transcription factor A (Tfam), which directly stimulates mitochondrial DNA replication and transcription [13-15]. Key steps in several exercise-induced pathways of the skeletal muscle involve the activation of AMP-activated protein kinase (AMPK), which has been shown to regulate the phosphorylation and activation of PGC-1α [16].

Ergogenic aids, such as vitamins, proteins, polyphenols, amino acids, creatine monohydrates, and herbs, help improve physical performance, delay fatigue, enhance energy production, regulate oxidative stress, and accelerate metabolic activity [17-19]. *Gynostemma pentaphyllum* (Thumb.) Makino has been widely used as a traditional tea or herb medicine in Asia, including China, South Korea, and Japan. *G. pentaphyllum* is used to treat various diseases, including hepatitis, diabetes, and cardiovascular diseases [3]. Additionally, it reportedly elicits various effects and possesses numerous pharmacological properties, such as anti-inflammatory, lipid metabolism-regulatory, anti-diabetic, neuroprotective, and anti-obesity properties [20-27]. Dammarane gypenosides are considered the major bioactive constituents in *G. pentaphyllum* and possess hepatoprotective, antioxidant, anti-obesity, anti-inflammatory, hypolipemic, hypoglycemic, and anticancer properties [21,28-31]. Moreover, polysaccharides or gypenosides from *G. pentaphyllum* have been investigated for their anti-fatigue and anti-oxidative activities [32,33]. Previously, we demonstrated the anti-obesity effect of *G. pentaphyllum* extract (GPE) and gypenoside L (GL), a saponin isolated from *G. pentaphyllum.* Both GPE and GL boosted glucose uptake and GLUT4 expression via activation of the AMPK-acetyl-CoA carboxylase (ACC) signaling pathway and promoted mRNA expression of *Ppargc1a* in skeletal muscle cells [34]. However, whether GPE and GL regulate the mitochondrial biogenic pathway via PGC-1α expression in C2C12 myotubes remains unclear.

Thus, we hypothesized that GPE and its active compound GL activate the PGC-1α pathway and regulate various genes associated with exercise performance, such as those governing muscle differentiation, muscle fiber switching, lactate metabolism, and energy metabolism. To this end, we investigated the effect of GPE and GL on muscle differentiation and mitochondrial metabolism in murine C2C12 myotubes.

MATERIALS AND METHODS

Chemicals and reagents

Creatine monohydrate was purchased from Sigma-Aldrich Co. (St. Louis, MO, USA). Dulbecco's modified Eagle's medium (DMEM), fetal bovine serum (FBS), penicillin/streptomycin solution, horse serum (HS), and phosphate-buffered saline (PBS) were obtained from GIBCO BRL Life Technologies (Grand Island, NY, USA). Primary anti-AMPKα (total or phosphor-form), anti-SIRT1 (total or phosphor-form), and anti-p38 (total or phosphor-form) antibodies, as well as secondary antibodies against anti-rabbit and anti-mouse immunoglobulin G (IgG) horseradish peroxidase (HRP)-linked antibodies, were obtained from Cell Signaling Technology (Beverly, MD, USA). Anti-Myh1 and anti-NRF2 (total or phosphor-form) antibodies were obtained from Abcam (Abcam Inc., Cambridge, UK). PGC-1α and glyceraldehyde 3-phosphate dehydrogenase (GAPDH) were purchased from Santa Cruz Biotechnology (Santa Cruz, CA, USA). MitoTracker® Red CMXRos and ProLong™ Gold Antifade Mountant with 4′,6-diamidino-2-phenylindole (DAPI) were purchased from Invitrogen (Carlsbad, CA, USA).

Preparation of GPE

G. pentaphyllum was purchased from Hunan Tea Group Co., Ltd (Changsha, Hunan, China), and a voucher specimen (20210301-1) was identified by Professor Zhou Ribao, College of Medicine, Hunan University of Traditional Chinese Medicine. The GPE and GL were prepared at BTC Corporation, according to a previously described method [34]. In brief, 1 kg of dried *G. pentaphyllum* leaves were extracted with a hot water (20 L) and 50% EtOH aqueous solution (15 L). After each extraction, the extracts were combined, concentrated, and filtered. Quantification of GL in GPE was performed using high-performance liquid chromatography (HPLC) with a diode-array detector. GPE contains active components such as GL (1.8%, w/w), gypenoside LI (GLI) (1.4%, w/w), and ginsenoside Rg3 (0.15%, w/w). A representative chromatogram of the standard references and the corresponding peaks in the GPE are presented in **Supplementary Figs. 1** and **2**.

Cell culture and treatment procedures

Murine C2C12 myoblast cells were purchased from American Type Culture Collection (Manassas, VA, USA). The C2C12 myoblasts were cultured and maintained in growth medium consisting of DMEM supplemented with 10% (*v/v*) FBS and 1% (*v/v*) penicillin/streptomycin solution under a humidified atmosphere of 95% air and 5% CO_2 at 37°C. For differentiation induction, C2C12 myoblasts at 85–95% confluence were incubated in differentiation medium with DMEM containing 2% (*v/v*) HS every 2 days. The obtained C2C12 myotubes were treated with/without GPE (20 μg/mL) or GL (0.36 μg/mL). Creatine monohydrate (CrM, 5 μg/mL) was used as a positive control. All controls were incubated with equal volumes of the vehicles used for the GPE, GL, and CrM treatments.

Quantitative reverse transcription polymerase chain reaction assay (qRT-PCR)

After 4 days of cell differentiation, total RNA was isolated by using an RNeasy® Plus Mini kit (Qiagen, Valencia, CA, USA) according to the manufacturer's instructions. First-strand

reverse transcription was performed with 2 μg total RNA using a Hyperscript™ RT master mix kit (GeneAll Biotechnology, Seoul, Korea). The levels of transcripts were determined by performing qRT-PCR on a Rotor-Gene 3000 instrument (Corbett Research, Mortlake, Australia) and using a Rotor-Gene™ SYBR Green Kit (Qiagen) as a double-stranded DNA-specific dye, according to the manufacturer's instructions. The primers used in the present study were ordered from and synthesized by Bioneer Co. (Daejeon, Korea); their sequences are listed in **Table 1**. The qRT-PCR consisted of 41 cycles, comprising 1 cycle of 3 min at 94°C and 40 cycles of 10 s at 95°C, 15 s at 60°C, and 20 s at 72°C. The amount of mRNA expression was normalized with the housekeeping gene *Gapdh* to determine the relative expression ratios for each mRNA gene expression relative to the control group. For statistical analysis purposes, all experiments included a minimum of three independent PCR reactions.

Western blot analysis

After 7 days of differentiation, cells were washed, harvested, and lysed with an ice-cold lysis buffer (20 mM HEPES pH 7.5, 150 mM NaCl, 1 mM EGTA, 1 mM EDTA, 100 mM NaF, 10 mM sodium pyrophosphate, and 1% Triton X-100) containing 0.2 mM PMSF, 5 mM iodoacetic acid, and a phosphatase/protease inhibitor (iNtRON Biotechnology, Inc., Seongnam, Korea). The lysates were collected, and protein concentrations were quantified using a BCA protein assay kit (Thermo Scientific, Rockford, IL, USA). Equal amounts of protein (50 μg) were separated by 10% (*v/v*) Sodium dodecyl sulphate-polyacrylamide gel electrophoresis and transferred onto polyvinylidene fluoride nitrocellulose membranes by electroblotting. The membrane blots were blocked overnight at 4°C in blocking buffer (5% skim milk in Tris-buffered saline with 0.1% Tween-20 [TBST]) and incubated with the following primary

Table 1. Primer sequences used in qRT-PCR for the analysis of mRNA expression

Genes	Accession No.	Primer sequences (5′→3′)
Myh1 (type IIx)	XM_021411424.2	Forward: GCTGGAAGATGAGTGCTCAGAG
		Reverse: TCCAAACCAGCCATCTCCTCTG
Myh7 (type I)	XM_017315841.2	Forward: CGCTCCACGCACCCTCACTT
		Reverse: GTCCATCACCCCTGGAGAC
Myh2 (type IIa)	XM_021176019.2	Forward: CCATTCAGAGCAAAGATGCAGGG
		Reverse: GCATAACGCTCTTTGAGGTTG
Myh4 (type IIb)	XM_021175597.1	Forward: GCTAGGGTGAGGGAGCTTGAA
		Reverse: AGACCCTTGACGGCTTCGA
Pparg1α	XM_006503779.4	Forward: GTC CTT CCT CCA TGC CTG AC
		Reverse: GAC TGC GGT TGT GTA TGG GA
Ldhb	NM_001316322.1	Forward: CCT CAG ATC GTC AAG TAC AGC C
		Reverse: ATC CGC TTC AAA TCA CAC GGT G
Esrrα	NM_007953.2	Forward: TTC GGC GAC TGC AAG CTC
		Reverse: CAC AGC CTC AGC ATC TTC AAT G
Mct1	XM_021196222.2	Forward: GCT GGG CAG TGG TAA TTG GA
		Reverse: CAG TAA TTG ATT TGG GAA ATG CAT
Fndc5	XM_006503212.4	Forward: ATG AGG TGA CCA TGA AGG AGA TGG C
		Reverse: CTG GTT TCT GAT GCG CTC TTG GTT
Gys1	NM_030678.3	Forward: CAC AGA ACG GTT GTC GGA CTT G
		Reverse: AGG TGA AGT GGT CTG GAA AGG C
Cpt1b	NM_009948.2	Forward: CCT GGA AGA AAC GCC TGA TT
		Reverse: CAG GGT TTG GCG AAA GAA GA
Ucp2	NM_011671.5	Forward: CTCGTCTTGCCGATTGAAGGT
		Reverse: TCTGCAATGCAGGCAGCTGTC
Ucp3	NM_009464.3	Forward: GCC TAC AGA ACC ATC GCC AG
		Reverse: GCC ACC ATC TTC AGC ATA CA
Sod2	NM_013671.3	Forward: ATC AGG ACC CAT TGC AAG GA
		Reverse: AGG TTT CAC TTC TTG CAA GCT

qRT-PCR, quantitative reverse transcription polymerase chain reaction.

antibodies: Myh1, p-AMPK α (Thr172), AMPKα, p-p-38, p-38, p-SIRT1, SIRT1, PGC-1α, p-NRF2, NRF2, and GAPDH, (1:1,000, in 5% skim milk in TBST). The blots were washed thrice with TBST and incubated with a horseradish peroxidase-conjugated anti-rabbit IgG HRP-linked or anti-mouse IgG HRP-linked antibody (1:5,000, in 5% skim milk in TBST). Subsequently, the signal was visualized using an enhanced chemiluminescence technique with the Luminata™ Forte Western Chemiluminescent HRP Substrate (Millipore, Billerica, MA, USA), according to the manufacturer's protocol. Band intensity was quantified using an ImageQuant™ LAS 500 imaging system (GE Healthcare Bio-Sciences AB, Uppsala, Sweden).

Confocal microscopy and immunocytochemistry

C2C12 myoblasts (2×10^4 cells/mL) were seeded on an ibiTreat μ-Slide 8-well polymer coverslip (Ibidi GmbH, Martinsried, Germany) and differentiated using a common culture method. After differentiation with GPE, GL, or CrM, the coverslips were washed with 1× PBS and fixed with 4% formaldehyde/PBS for 15 min at room temperature, after which the myotubes were permeabilized with 0.5% Triton X-100 in PBS for 15 min. After washing thrice with 1× PBS, the myotubes were blocked with 3% bovine serum albumin in 1× PBS for 1 h at room temperature and immunostained with Myh1 primary antibody (1:3,000) overnight at 4°C. The coverslips were labeled with AlexaFlour® 488 goat anti-rabbit IgG secondary antibody (1:100) for 1 h at room temperature. MitoTracker® Red CMXRos and ProLong™ Gold Antifade Mountant with DAPI (Invitrogen) prepared in PBS were added at final concentrations of 50 nM and 1 μM, respectively. Myh1 expression was visualized by fluorescence microscopy (LSM 800; Carl Zeiss, Jena, Germany).

Measurement of mitochondrial reactive oxygen species (ROS) production

The intracellular production of ROS in C2C12 myotubes was assayed using the 2′7′-dichlorofluorescein diacetate (DCF-DA) assay, as previously described [35]. C2C12 myoblasts were cultured for 24 h in a 96-well plate and treated with or without GPE, GL, or CrM for 1 h. Myotubes were washed once with PBS and then incubated for 3 h with 50 μM tert-butyl hydrogen peroxide (tBHP). Cells were washed with PBS and stained with 20 mM DCF-DA for 45 min. The level of DCF fluorescence was detected by a fluorescence reader at excitation/emission wavelengths of 495 nm/529 nm. Data are presented as relative fluorescence units/well.

Statistical analysis

All data represent five replicate independent experiments. Statistical analysis of the collected data was performed using GraphPad Prism (GraphPad Prism Software Inc., La Jolla, CA, USA). All values are expressed as the mean ± SE. Statistical analyses were performed using the Student's *t*-test or performing a one-way analysis of variance. *P*-value < 0.05 was considered indicative of a statistically significant difference.

RESULTS

Treatment with GPE and GL enhance myoblast differentiation

To investigate the role of GPE and GL in myoblast differentiation, we first examined their effects on cell viability during a 4-day differentiation period. The concentrations of GPE and GL used in the treatment manifested no cytotoxic effects in C2C12 myotubes (**Fig. 1**). This was further confirmed by using qRT-PCR to assess the mRNA expression of specific markers (*Myh1, Myh7, Myh2,* and *Myh4*). There was a noticeable increase in the *Myh1* mRNA expression level in cells
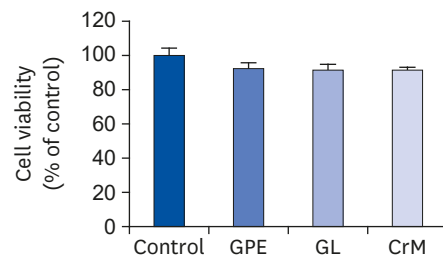
Fig. 1. Cell-toxicity analysis result. C2C12 cells were incubated in differentiation medium with GPE, GL, or CrM for 4 days. MTT assays showed no cytotoxic effects from the GPE, GL, and CrM treatments in C2C12 cells. All data represent five replicates (n = 5), and values are shown as means ± SE.
GPE, *Gynostemma pentaphyllum* extract; GL, gypenoside L; CrM; creatine monohydrate.

treated with GPE and GL compared to that of control cells (**Fig. 2A**). The mRNA expression level of *Myh1* following treatment with GPE and GL was also higher than that observed following treatment with CrM. Similarly, the *Myh7* expression level was significantly elevated in cells treated with GPE and CrM (**Fig. 2B**); however, the expression level of the CrM group was higher than that of the GPE group. In addition, GPE, GL, and CrM caused an elevation in the mRNA levels of *Myh2* in C2C12 myotubes (**Fig. 2C**), but there was no significant difference among the groups. By contrast, the *Myh4* mRNA expression level showed a significant reduction following GPE treatment (**Fig. 2D**). We next performed western blot analysis to examine the effects of GPE and GL on differentiation in C2C12 cells. As presented in **Fig. 3A**, myoblast cells, following treatment with GPE and GL, exhibited a gradual morphological change into an elongated shape and formed mature multi-nucleated myotubes. The GPE-treated cells showed increased Myh1 protein expression levels (**Fig. 3B**). Immunocytochemistry confirmed that treatment with GPE and GL augmented Myh1 expression, with a resultant elongated and widened cylindrical cell
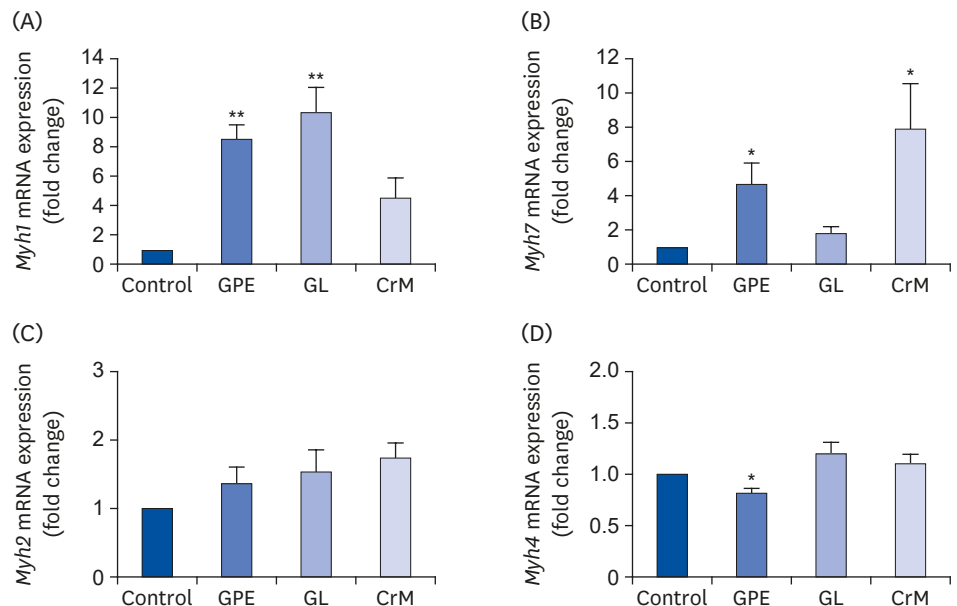
Fig. 2. Effect of GPE and GL on the mRNA expression of MyHC genes in C2C12 myotubes. C2C12 cells were incubated in differentiation medium with GPE, GL, or CrM for 4 days. The mRNA expression levels of *Myh1* (A), *Myh7* (B), *Myh2* (C), and *Myh4* (D) were determined by qRT-PCR. All data represent five replicates (n = 5), and values are shown as means ± SE.
GPE, *Gynostemma pentaphyllum* extract; GL, gypenoside L; CrM, creatine monohydrate.
*$P < 0.05$ and **$P < 0.01$ indicate a significant difference from the control group.

shape (**Fig. 3C**). The fluorescence signals from MitoTracker and Myh1 were quantified using Image J software. The fluorescence intensity of MitoTracker showed values similar to those of the treatment group cells. The fluorescence signal intensity increased with the stage of progression of muscle differentiation. The signals emitted from GPE-treated cells were significantly
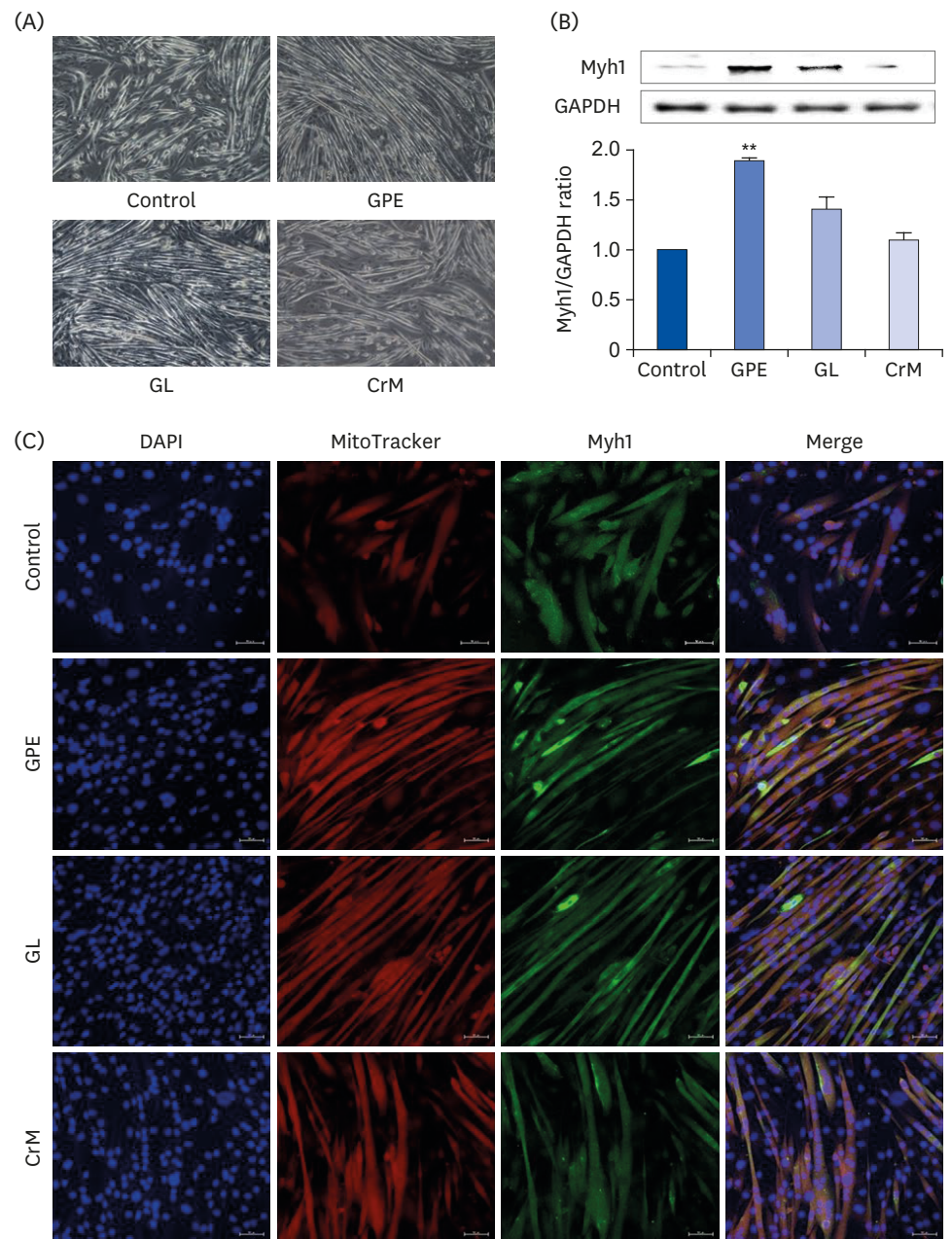

Fig. 3. Effect of GPE and GL on the differentiation of myoblasts into myotubes. (A) C2C12 cells were incubated in differentiation medium with GPE, GL, or CrM for 4 (immunofluorescence staining) and 7 (western blot) days. (B) Protein expression of Myh1 was assessed by western blotting analysis. GAPDH was used as a loading control. All data represent five replicates (n = 5), and values are shown as means ± SE. (C) Immunofluorescence staining of Myh1 in C2C12 myotubes. The cells were fixed and immunostained for Myh1 (green), MitoTracker (red), and DAPI (blue). Myotube formation was observed by fluorescence microscopy (original magnification, 200×) (scale bar = 50 μm). GPE, *Gynostemma pentaphyllum* extract; GL, gypenoside L; CrM, creatine monohydrate; GAPDH, glyceraldehyde 3-phosphate dehydrogenase; DAPI, 4',6-diamidino-2-phenylindole.
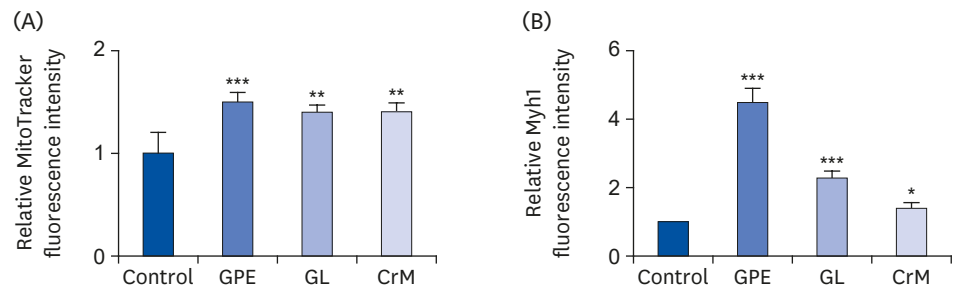**P < 0.01 indicate a significant difference from the control group.

(A)

(B)

Fig. 4. Quantification of MitoTracker and Myh1 staining intensity in C2C12 cells. Differentiated C2C12 cells at day 4 were stained with MitoTracker (A) and Myh1 (B). Fluorescence intensity of immunofluorescence sections was quantified using Image J software. The results are expressed as means ± SEM (n = 5).
SEM, standard error of the mean; GPE, *Gynostemma pentaphyllum* extract; GL, gypenoside L; CrM, creatine monohydrate.
*$P < 0.05$, **$P < 0.01$, and ***$P < 0.001$ indicate a significant difference from the control group.

stronger than those emitted from GL- and CrM-treated cells (**Fig. 4A and B**). Taken together, these results demonstrated that GPE and GL augment the expression of differentiation markers in C2C12 cells.

Effect of GPE and GL on lactate metabolism
To investigate the influence of GPE and GL on the molecular mechanism involved in lactate metabolism, we performed qRT-PCR. As shown in **Fig. 5A**, GPE and GL significantly augmented the mRNA expression of *Ppargc1a* by 8.18-fold and 11.75-fold, respectively, compared to the corresponding expression level in control myoblasts. C2C12 cells were treated with GPE and GL to examine the effect of GPE and GL on fatigue-related genes

(A)

(B)

(C)

(D)
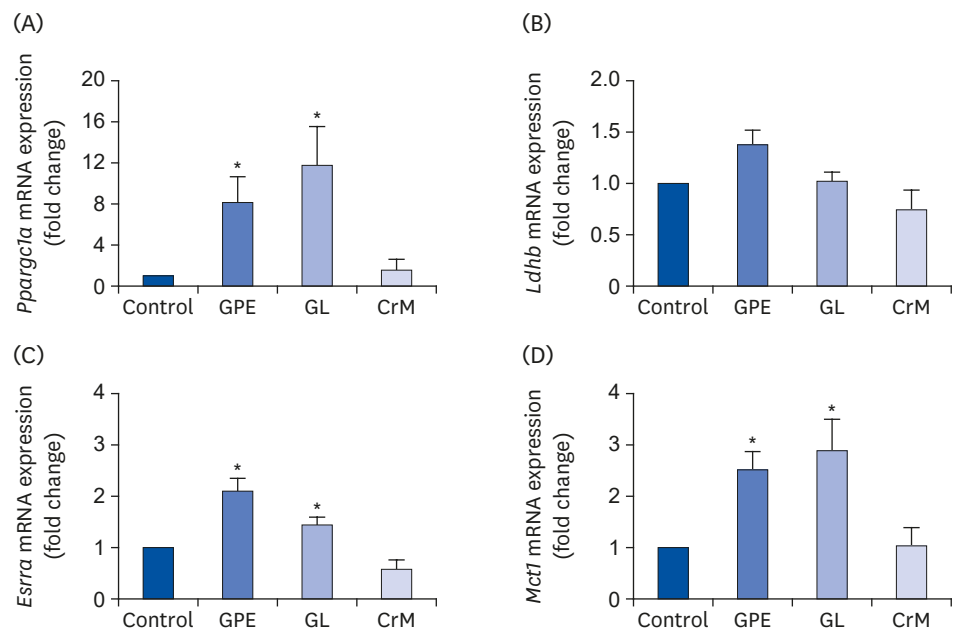
Fig. 5. Effects of GPE and GL on lactate metabolism in C2C12 myotubes. Differentiated C2C12 myotubes were treated with/without GPE, GL, or CrM. The mRNA expression levels of *Ppargc1a* (A), *Ldhb* (B), *Esrra* (C), and *Mct1* (D) were evaluated by qRT-PCR. Target gene expression levels were normalized to the *Gapdh* expression level. Data are expressed as means ± SE (n = 5).
GPE, *Gynostemma pentaphyllum* extract; GL, gypenoside L; CrM, creatine monohydrate; qRT-PCR, quantitative reverse transcription polymerase chain reaction.
*$P < 0.05$ indicate a significant difference from the control group.

encoding lactate dehydrogenase (LDH)-B, ERRα, and monocarboxylate transporter (MCT) 1, which regulate lactate production and clearance in myotubes [36]. As shown in **Fig. 5B-D**, we determined that GPE and GL treatment markedly increased *Esrra* and *Mct1* mRNA expression; however, it resulted in a non-significant increase in *Ldhb* mRNA expression. These results indicated that GPE regulates lactate metabolism by promoting *Esrra* and *Mct1* expression.

Effects of GPE and GL on mitochondrial metabolism

We investigated whether GPE and GL regulate metabolic genes at the transcriptional level. As shown in **Fig. 6**, treatment of C2C12 myotubes with GPE and GL resulted in a significant elevation in the mRNA expression levels of fibronectin type III domain-containing protein 5 (*Fndc5*) (**Fig. 6A**), which is related to adipocyte browning, and glycogen synthase (*Gys*) (**Fig. 6B**). Furthermore, we observed that GPE and GL promote lipid metabolism by increasing the mRNA expression of carnitine palmitoyltransferase 1b (*Cpt1b*); however, only GPE produced a nearly 3-fold increase and a statistically significant difference compared to the corresponding parameters in untreated cells (**Fig. 6C**).

Effect of GPE and GL on AMPK activation

To further elucidate the molecular mechanism(s) underlying the GPE- and GL-induced changes in muscle metabolism, we evaluated their effects on the AMPK pathway. As shown in **Fig. 7A**, treatment with GPE significantly increased the phosphorylation of the AMPK α-subunit at Thr172, which is within the active site of the AMPK-α subunit. In addition, GPE and GL activated p38 MAPK, a critical regulator of glucose uptake (**Fig. 7B**) [37]. Our previous results indicated that GPE and GL mediate glucose metabolism and metabolic functions via
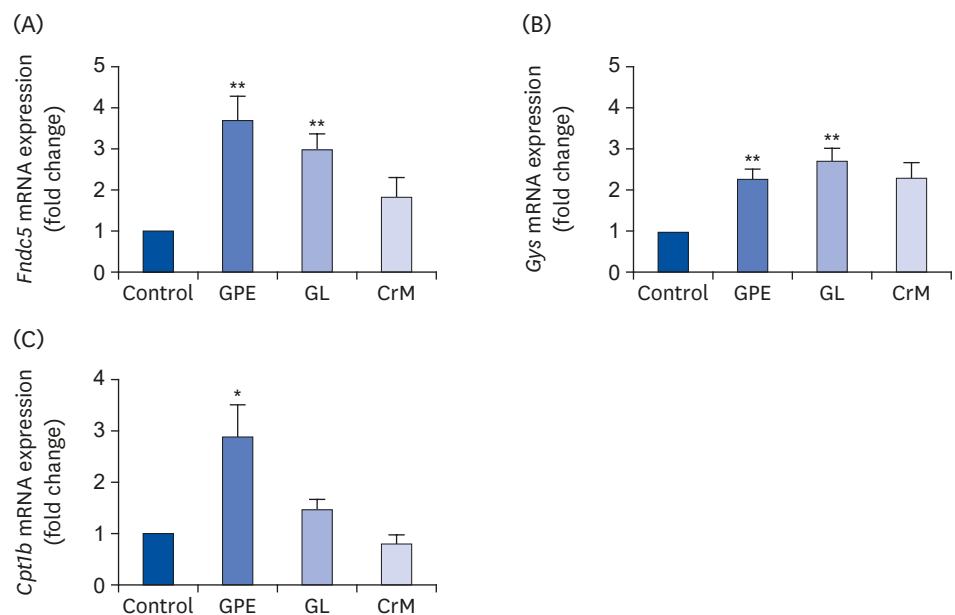
Fig. 6. Effects of GPE and GL on adipocyte browning, glycogen synthesis, and lipid metabolism in C2C12 myotubes. Differentiated C2C12 myotubes were treated with GPE, GL, or CrM for 4 days. The mRNA expression levels of genes related to adipocyte browning (*Fndc5*) (A), glycogen synthesis (*Gys*) (B), and lipid metabolism (*Cpt1b*) (C) were determined by qRT-PCR. Target gene expression levels were normalized to the *Gapdh* expression level. Each value represents the mean ± SE (n = 5).
GPE, *Gynostemma pentaphyllum* extract; GL, gypenoside L; CrM, creatine monohydrate; *Fndc5*, fibronectin type III domain-containing protein 5 gene; *Gys*, glycogen synthase gene; qRT-PCR, quantitative reverse transcription polymerase chain reaction.
*$P < 0.05$ and **$P < 0.01$ indicate a significant difference from the control group.

Fig. 7. Effect of GPE and GL on the AMPK/p38 MAPK/SIRT1/PGC-1α signaling pathway. C2C12 cells were cultured for 4 days in differentiation medium supplemented w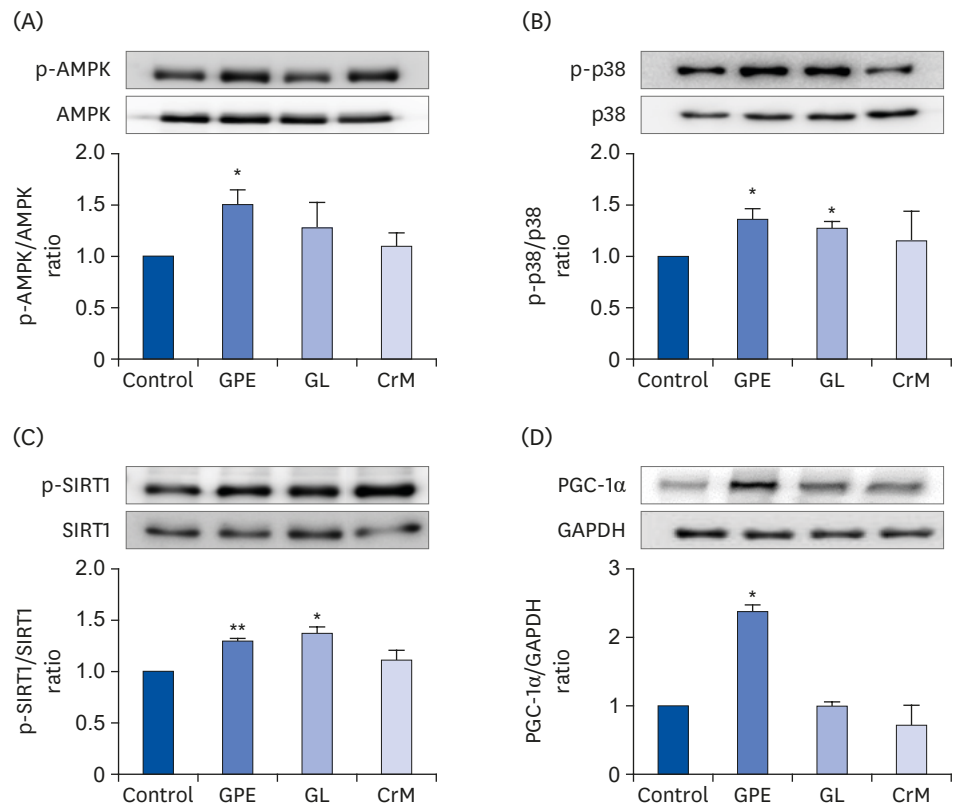ith/without GPE, GL, or CrM. The ratios of p-AMPK/AMPK (A), p-p38/p38 (B), p-SIRT1/SIRT1(C), and PGC-1α/GAPDH (D) were determined. Each bar represents the mean ± SE (n = 5) relative to the control group.
GPE, *Gynostemma pentaphyllum* extract; GL, gypenoside L; CrM, creatine monohydrate; AMPK, AMP-activated protein kinase; PGC-1α, peroxisome proliferator-activated receptor-gamma co-activator 1α; GAPDH, glyceraldehyde 3-phosphate dehydrogenase.
*$P < 0.05$ and **$P < 0.01$ indicate a significant difference from the control group.

AMPK and p38 MAPK phosphorylation [38]. Activation of AMPK reportedly increases SIRT1 expression in skeletal muscles [39], while AMPK directly phosphorylates and activates PGC-1α by SIRT1, which deacetylates the lysine-site of PGC-1α and activates downstream genes related to energy expenditure [40]. Herein, we determined that treatment with GPE and GL in C2C12 myotubes resulted in increased protein levels of phosphorylated SIRT1 (**Fig. 7C**) and PGC-1α (**Fig. 7D**). Consequently, it was inferred that the effects of GPE and GL are mediated via the activation of AMPK/p38, SIRT1, and PGC-1α.

Effect of GPE and GL on oxidative stress-related gene expression
We next examined whether GPE and GL protect muscle cells from oxidative stress by activating related gene expression. In **Fig. 8A and B**, it is shown that treatment with GPE and GL significantly induced the mRNA expressions of the fatty acid metabolism/mitochondrial biogenesis markers, uncoupling protein (UCP) 2 (*Ucp2*) and 3 (*Ucp3*). The endogenous antioxidant response element *Sod2* was also significantly upregulated, by approximately 1.6-fold following treatment of myotubes with GL (**Fig. 8C**). Given that NRF2 phosphorylation at Ser40, which is induced by several kinases, is a crucial process in its nuclear translocation [41-43], we investigated the phosphorylation of NRF2 by performing western blot analysis. The results shown in **Fig. 8D** indicated that the ratio of NRF2 phosphorylation/total NRF2
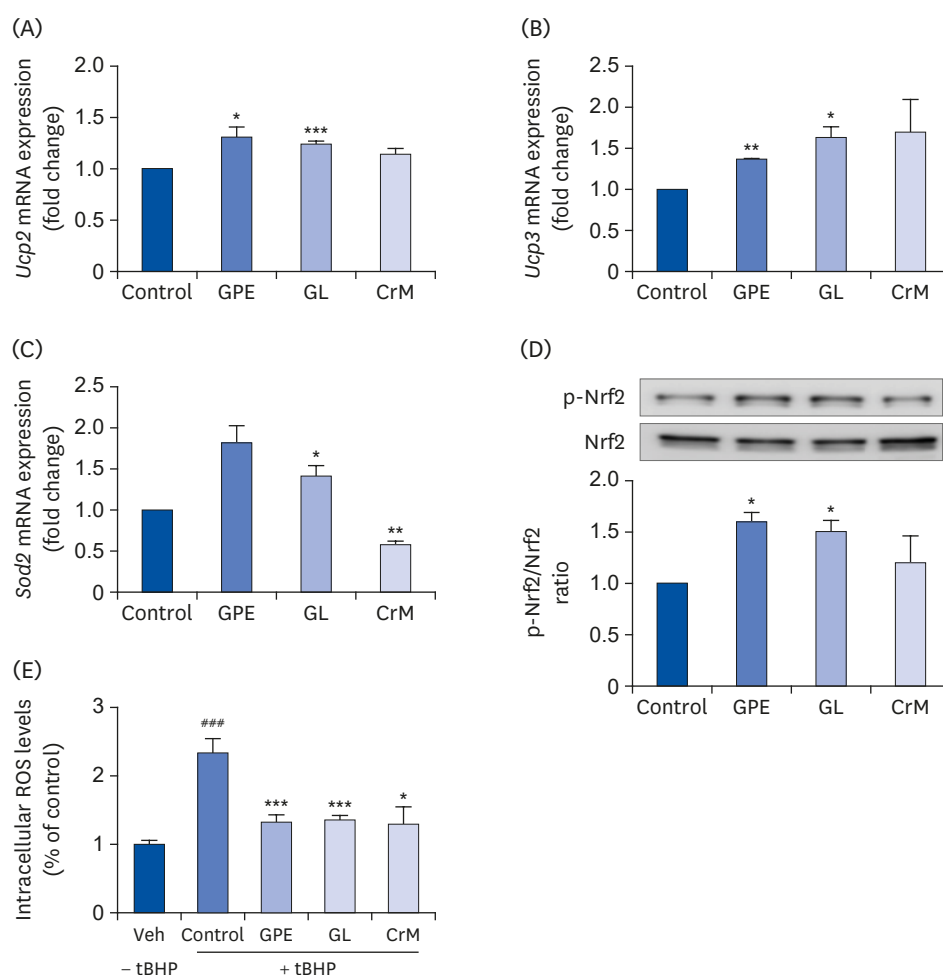
Nutrition
Research and
Practice

Fig. 8. Effect of GPE and GL on the relative mRNA expression level of oxidative stress-related genes in C2C12 myotubes. C2C12 cells were treated with GPE, GL, or CrM for 4 days. The mRNA levels of *Ucp2* (A), *Ucp3* (B), *Sod2* (C), and the protein levels of phosphorylated NRF2 and NRF2 (D) were analyzed by qRT-PCR and western blot assay, respectively. *Gapdh* served as an internal control. The ratio of p-NRF2/NRF2 was determined. (E) Effects of GPE and GL on ROS levels in C2C12 myotubes. Cells were studied under normal conditions (Veh), treatment with tBHP for 3 h (Control), and combinations of tBHP with GPE, GL or CrM. ROS levels are presented as fold changes from control cells. All values are presented as the mean ± SE (n = 5).
GPE, *Gynostemma pentaphyllum* extract; GL, gypenoside L; CrM, creatine monohydrate; NRF, nuclear respiratory factor; qRT-PCR, quantitative reverse transcription polymerase chain reaction; ROS, reactive oxygen species; tBHP, tert-butyl hydrogen peroxide.
*$P < 0.05$, **$P < 0.01$, and ***$P < 0.001$ indicate a significant difference from control group. ###$P < 0.001$ Indicate significant difference from tBHP alone.

was markedly increased following treatment with GPE and GL. The effects of GPE and GL on oxidative stress protective mechanisms are likely mediated by an intrinsic antioxidant capacity. Thus, we investigated whether GPE and GL indeed mediate oxidative stress in muscle cells by assessing ROS generation. Intracellular ROS was detected with DCF-DA, as shown in **Fig. 8E**. In C2C12 myotubes, tBHP treatment significantly increased intracellular ROS by 2.3-fold compared to the ROS level recorded in control cells. However, when the tBHP-treated C2C12 cells were stimulated with GPE and GL, the ROS levels were significantly reduced (**Fig. 8E**), indicating that GPE and GL treatments induce an intracellular anti-oxidative response.

DISCUSSION

G. pentaphyllum has been reported to exert anti-inflammatory, lipid metabolism-regulatory, anti-diabetic, neuroprotective, and anti-obesity effects [20-27,34]. Gypenosides are a class of major bioactive compounds in GPE and have been evaluated for their beneficial cholesterol-lowering, antioxidant, hypoglycemic, and tumor-suppressive effects [44-47]. Gypenosides or polysaccharides from *G. pentaphyllum* help improve exercise tolerance, extend swimming time, prevent the rise in lactate levels, and mitigate oxidative stress during exhaustive exercise [32,33]. However, the mechanisms of action of GPE and GL on muscle differentiation and mitochondrial metabolism in C2C12 myotubes remain inadequately described. The L6 and C2C12 myoblast cell lines (rat and mouse, respectively) are commonly used to evaluate myocellular metabolism and the regulatory processes involved in myogenesis. In a previous study, GPE enhanced glucose uptake, which was mediated by the AMPK and ACC signaling pathway, and also increased the gene expression of *SIRT1* and *PGC-1α* in L6 cells [34]. In the present study, we evaluated the beneficial effects of GPE and GL, demonstrated by their association with increased myoblast differentiation, lactate metabolism, adipocyte browning, glycogen synthase, and anti-oxidative stress effects; these, in turn, are associated with the upregulation of genes and proteins related to the activated AMPK pathway in C2C12 skeletal muscle myotubes treated with the study compounds.

The compounds GL, GLI, and Rg3 are present at 1.8, 1.4, and 0.15 mg, respectively, per gram of GPE. Moreover, GL, GLI, and Rg3 are present in small quantities in raw *G. pentaphyllum* plants. GPE obtained by a newly patented extraction method contains large amounts of GL, GLI, and Rg3. In this study, we investigate the effects of both GPE and GL; regardless, it is also necessary to investigate the effects of GLI and Rg3 on mitochondrial metabolism. Interestingly, a study using a Caco-2 cell monolayer permeability model showed Caco-2 cell permeability of saponins from *G. pentaphyllum*, indicated the potential oral bioavailability of dammarane saponins from *G. pentaphyllum* [48]. The study indicated that GL exhibited a high permeability across Caco-2 monolayers, whereas GLI showed a 10-fold decrease in permeability, demonstrating the effects of the bioactive compound GL obtained from *G. pentaphyllum*. Therefore, our results suggest that GPE containing GL may have a potential for application in the production of nutraceuticals, functional foods, and food additives.

Skeletal muscle is the most plentiful tissue in the human body. It supports physiological conditions [49] and possesses a remarkable ability for regeneration following severe cell damage resulting from exercise, injury, or disease [50]. As skeletal muscle-derived stem cells, satellite cells are the basal source for myogenesis and undergo differentiation into myocytes to repair myofibers following activation by muscle injury. Satellite cells initiate myogenic differentiation and constitute their own satellite cell pool through self-renewal, which is necessary for continuous muscle regeneration [51]. In the present study, treatment of C2C12 myotubes with GPE and GL markedly promoted the differentiation and expression of Myh1 at both the mRNA and protein levels. Furthermore, the immunostaining results showed that GPE and GL treatments led to the fusion of myoblasts into multi-nucleated myotubes, as determined by changes in cell morphology and Myh1 expression. Treatment with CrM remarkably stimulated *Myh7* mRNA expression levels, which were much higher than those of GPE-treated cells. However, GPE, GL, and CrM did not influence *Myh2* mRNA expression in C2C12 myotubes, and GPE treatment caused a significant reduction in the *Myh4* mRNA expression level. Zhang *et al.* [7] reported that PGC-1α transgenic mice and pigs manifested increased transcriptional induction of oxidative fiber markers, such as Myh7,

Myh1, myoglobin, and TNNI1, with reduced expression levels of several glycolytic fiber genes (*Myh2, Myh4, Casq1,* and *Tnni2*). In the present study, GPE significantly augmented the *Myh1* and *Myh7* expression levels but not those of *Myh2* and *Myh4.* These results showed that GPE treatment of C2C12 myotubes leads to the transformation of muscle fiber from a glycolytic type to an oxidative type. Therefore, an increased oxidative potential by treatment with GPE may help improve endurance performance and resistance to fatigue.

PGC-1α is a key transcriptional regulator of several genes involved in adjustment to exercise, such as those involved in lactate and fatty acid metabolism, antioxidant defense, muscle growth, and mitochondrial biogenesis [5,52-54]. In skeletal muscle, PGC-1α has also been shown to regulate muscle fiber switch, lipid oxidation, glucose uptake, and lactate catabolism. Lactate is considered an immediate energy source and an energy reserve contributor. PGC-1α controls lactate levels by promoting LDH-B conversion of lactate to pyruvate, and MCT1 expedites lactate uptake. The increase in *Ldhb* mRNA expression following GPE and GL treatment indicates the downregulation of lactate production when PGC-1α binds to an ERR-responsive element in the *Ldhb* promoter. Additionally, MCT1 expression is reportedly enhanced by PGC-1α. The activation of ERRα by PGC-1α promotes the transcription of MCT1, which directs lactate into muscle cells. In the current study, GPE and GL also upregulated *Esrra* and *Mct1* mRNA expressions, implying that an increase in PGC-1α expression in the muscles induced by GPE and GL enhances lactate metabolism.

PGC-1α expression in skeletal muscle contributes to managing energy balance, which promotes energy expenditure. Recent studies demonstrated that PGC-1α expression in muscle induces an increase in the expression of fibronectin type III domain containing 5 (FNDC5) [15]. Irisin, one of the most important thermogenic adipomyokines secreted by FNDC5 cleavage, is involved in the browning of white fat cells and thermogenesis by activating UCP1. Irisin stimulates UCP1 expression and is positively regulated by PGC-1α [55]. Farahabadi *et al.* [56] reported that vitamin A increases FNDC5 gene expression via the extracellular signal-regulated kinases (ERK) 1/2-cAMP response element-binding protein (CREB)-PGC-1α-FNDC5 pathway. Chen *et al.* [57] showed that icariin induces irisin/FNDC5 expression in skeletal muscles via the AMPK pathway. Liu *et al.* [58] reported that gypenosides significantly reduce high-fat diet-induced obesity and enhance white adipose tissue browning signaling, including PGC-1α, PRDM16, and UCP1. Herein, we provided the first demonstration that GPE and GL elevate *Fndc5* expression in C2C12 myotubes. After a period of exercise, AMPK is activated due to ATP consumption, which leads to acceleration in fatty acid β-oxidation, glucose uptake, and glucose phosphorylation, resulting in increased intracellular levels of glucose-6-phosphate (G6P) for ATP production [59,60]. The activity of glycogen synthase (GYS), the main regulatory enzyme in glycogen synthesis, is mediated by the allosteric activator G6P. In general, AMPK negatively regulates glycogen synthesis via phosphorylation and inactivation of GYS at site 2 [59]. Thus, stimulating AMPK would lower muscle glycogen levels by inhibiting GYS enzyme activity. Recent research has shown that although 5-aminoimidazole-4-carboxamide ribonucleotide (AICAR) mediates GYS inactivation, elevated glucose transport promoted by the activation of AMPK leads to an accumulation of intracellular G6P levels. Consequently, AMPK activation enhances glycogen synthesis by activating GYS through glucose transport [61,62]. We also observed that GPE and GL treatments increased the expression level of *Gys* mRNA in C2C12 myotubes. Furthermore, PGC-1α regulates lipid metabolism by stimulating the expression of *Cpt1b* target genes [63]. In the present study, we determined that GPE and GL may induce the upregulation of PGC-1α and help promote fatty acid metabolism.

PGC-1α is markedly activated by the immense energy demands of diverse physiologic and dietary conditions, and it interacts with several transcription factors. AMPK and SIRT1 signaling pathways influence PGC-1α activation directly through phosphorylation and deacetylation, respectively. In addition, p38 has an important role in activating the CREB/activating transcription factor 2 site on the PGC-1α gene promoter [38,64]. PGC-1α induces the expression of Tfam and the mitochondrial regulator NRF2, which is an essential intracellular antioxidant response factor that activates mitochondrial genes in the nucleus, resulting in upregulation of mitochondrial biogenesis [65]. In addition, PGC-1α enhances mitochondrial uncoupling by inducing UCP2 and UCP3 in the inner mitochondrial membrane. UCP2 and UCP3 mediate the upregulation of energy spending, fatty acid metabolism, and thermogenic uncoupling. It has also been demonstrated that UCP2 and UCP3 contribute protective effects against mitochondrial oxidative stress damage by reducing the generation of ROS. Recent studies suggested that PGC-1α regulates the expression of endogenous antioxidant proteins. PGC-1α enhances the uncoupling capacity of the mitochondria and activates ROS-scavenging enzymes such as superoxide dismutase 2 (SOD2), catalase, and GPx1 [53,66]. In the present study, we demonstrated that GPE and GL significantly increase the expression of UCP2, UCP3, SOD, and NRF2 nuclear translocation, which induces mitochondrial uncoupling and decreases ROS production. The induction of PGC-1α by GPE and GL signifies that PGC-1α activation is an instrumental factor in minimizing or preventing ROS production by upregulating the expression of antioxidant genes. **Fig. 9** summarizes the proposed mechanisms through which GPE and GL improve muscle differentiation and mitochondria metabolism in C2C12 myotubes. Although GPE
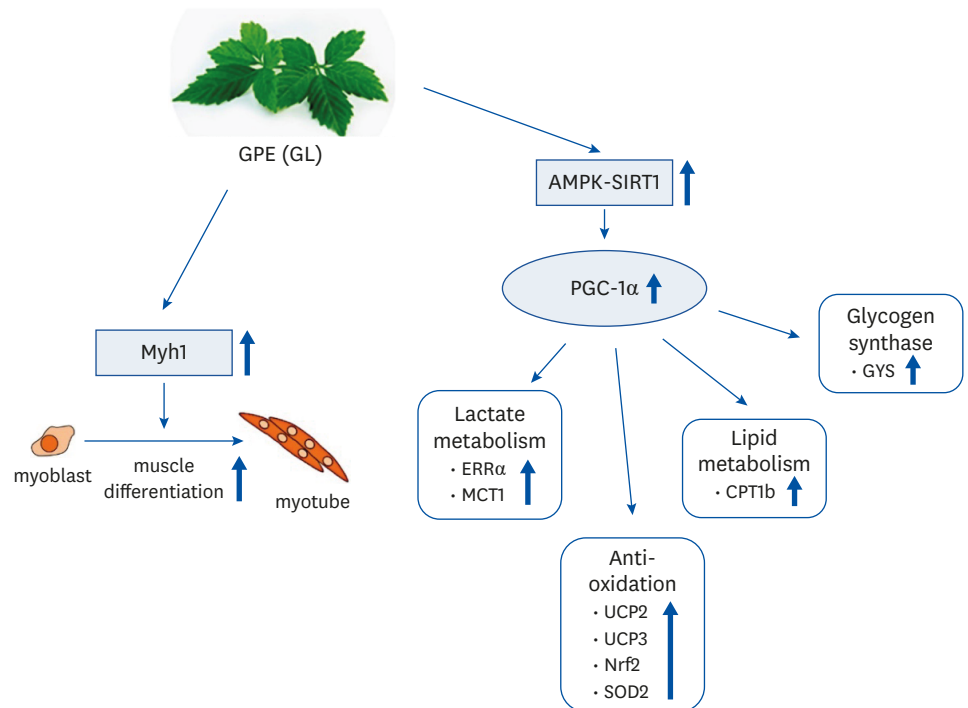

Fig. 9. Tentative mechanisms by which GPE and GL stimulate muscle differentiation and mitochondrial metabolism in C2C12 myotubes.
GPE, *Gynostemma pentaphyllum* extract; GL, gypenoside L; AMPK, AMP-activated protein kinase; PGC-1α, proliferator-activated receptor-gamma coactivator 1α; ERRα, estrogen-related receptor α; MCT1, monocarboxylate transporter 1; UCP, uncoupling protein; NRF, nuclear respiratory factor; SOD, superoxide dismutase; CPT, carnitine palmitoyl transferase; GYS, glycogen synthase.

and GL mediate the activation of the PGC-1α signaling pathway, the effect of mitochondrial biogenesis in C2C12 myotubes remains unclear. Furthermore, whether GPE and GL could improve exercise performance through endurance training remains largely undescribed and will require further investigation.

The results of our investigation demonstrated that treatment with GPE and GL promoted the differentiation of myoblasts into myotubes and elevated Myh1 expression in C2C12 cells. In addition, GPE and GL stimulated lactate metabolism, upregulated PGC-1α expression by activating the AMPK/p38/SIRT1 signaling pathway, and enhanced the anti-oxidative stress effect by promoting the expression of associated genes in skeletal muscle cells. Thus, our findings underscore the potential use of GPE and GL as candidates in the further development of sports dietary supplements aimed at enhancing the health benefits of exercise. Further studies are warranted to elucidate the underlying molecular mechanism driving the effects of GPE and GL on exercise endurance capacity in animal models.

ACKNOWLEDGMENTS

SUPPLEMENTARY MATERIALS

Supplementary Fig. 1

HPLC chromatogram (A) of GPE and LC-MS spectra (B) of noted HPLC peaks (i), (ii), and (iii) with retention times of 12.32, 12.45, and 13.06 min determining GL, GLI, and ginsenoside Rg3 with 801.41, 801.47, and 785.52 $[M+H]^+$, respectively.

Click here to view

Supplementary Fig. 2

Identification of compound 1 isolated from the GPE. HPLC spectra of GL standard (A) and compound 1 (i-GL) (B); ^1H NMR (C) and ^{13}C NMR (D) spectra of the i-GL compound corresponding to the structure isolated as GL.

Click here to view

REFERENCES

1. Papa EV, Dong X, Hassan M. Skeletal muscle function deficits in the elderly: current perspectives on resistance training. J Nat Sci 2017;3:e272.
   PUBMED

2. Egan B, Zierath JR. Exercise metabolism and the molecular regulation of skeletal muscle adaptation. Cell Metab 2013;17:162-84.
   PUBMED | CROSSREF

3. Zurlo F, Larson K, Bogardus C, Ravussin E. Skeletal muscle metabolism is a major determinant of resting energy expenditure. J Clin Invest 1990;86:1423-7.
   PUBMED | CROSSREF

4. Margolis LM, Pasiakos SM. Optimizing intramuscular adaptations to aerobic exercise: effects of carbohydrate restriction and protein supplementation on mitochondrial biogenesis. Adv Nutr 2013;4:657-64.
PUBMED | CROSSREF

5. Kang C, Chung E, Diffee G, Ji LL. Exercise training attenuates aging-associated mitochondrial dysfunction in rat skeletal muscle: role of PGC-1α. Exp Gerontol 2013;48:1343-50.
PUBMED | CROSSREF

6. Ashmore CR, Tompkins G, Doerr L. Postnatal development of muscle fiber types in domestic animals. J Anim Sci 1972;34:37-41.
PUBMED | CROSSREF

7. Zhang L, Zhou Y, Wu W, Hou L, Chen H, Zuo B, Xiong Y, Yang J. Skeletal muscle-specific overexpression of PGC-1α induces fiber-type conversion through enhanced mitochondrial respiration and fatty acid oxidation in mice and pigs. Int J Biol Sci 2017;13:1152-62.
PUBMED | CROSSREF

8. Ferraro E, Giammarioli AM, Chiandotto S, Spoletini I, Rosano G. Exercise-induced skeletal muscle remodeling and metabolic adaptation: redox signaling and role of autophagy. Antioxid Redox Signal 2014;21:154-76.
PUBMED | CROSSREF

9. Santos-Zas I, Cid-Díaz T, González-Sánchez J, Gurriarán-Rodriguez U, Seoane-Mosteiro C, Porteiro B, Nogueiras R, Casabiell X, Relova JL, Gallego R, et al. Obestatin controls skeletal muscle fiber-type determination. Sci Rep 2017;7:2137.
PUBMED | CROSSREF

10. Bourdeau Julien I, Sephton CF, Dutchak PA. Metabolic networks influencing skeletal muscle fiber composition. Front Cell Dev Biol 2018;6:125.
PUBMED | CROSSREF

11. Wu Z, Puigserver P, Andersson U, Zhang C, Adelmant G, Mootha V, Troy A, Cinti S, Lowell B, Scarpulla RC, et al. Mechanisms controlling mitochondrial biogenesis and respiration through the thermogenic coactivator PGC-1. Cell 1999;98:115-24.
PUBMED | CROSSREF

12. Tadaishi M, Miura S, Kai Y, Kano Y, Oishi Y, Ezaki O. Skeletal muscle-specific expression of PGC-1α-b, an exercise-responsive isoform, increases exercise capacity and peak oxygen uptake. PLoS One 2011;6:e28290.
PUBMED | CROSSREF

13. Kelly DP, Scarpulla RC. Transcriptional regulatory circuits controlling mitochondrial biogenesis and function. Genes Dev 2004;18:357-68.
PUBMED | CROSSREF

14. Lin J, Handschin C, Spiegelman BM. Metabolic control through the PGC-1 family of transcription coactivators. Cell Metab 2005;1:361-70.
PUBMED | CROSSREF

15. Puigserver P, Spiegelman BM. Peroxisome proliferator-activated receptor-γ coactivator 1 α (PGC-1 α): transcriptional coactivator and metabolic regulator. Endocr Rev 2003;24:78-90.
PUBMED | CROSSREF

16. McConell GK, Ng GP, Phillips M, Ruan Z, Macaulay SL, Wadley GD. Central role of nitric oxide synthase in AICAR and caffeine-induced mitochondrial biogenesis in L6 myocytes. J Appl Physiol (1985) 2010;108:589-95.
PUBMED | CROSSREF

17. da Silva W, Machado AS, Souza MA, Mello-Carpes PB, Carpes FP. Effect of green tea extract supplementation on exercise-induced delayed onset muscle soreness and muscular damage. Physiol Behav 2018;194:77-82.
PUBMED | CROSSREF

18. Liu Y, Liu C. Antifatigue and increasing exercise performance of *Actinidia arguta* crude alkaloids in mice. J Food Drug Anal 2016;24:738-45.
PUBMED | CROSSREF

19. Lee BR, Lee JH, An HJ. Effects of *Taraxacum officinale* on fatigue and immunological parameters in mice. Molecules 2012;17:13253-65.
PUBMED | CROSSREF

20. la Cour B, Mølgaard P, Yi Z. Traditional Chinese medicine in treatment of hyperlipidaemia. J Ethnopharmacol 1995;46:125-9.
PUBMED | CROSSREF

21. Gou SH, Huang HF, Chen XY, Liu J, He M, Ma YY, Zhao XN, Zhang Y, Ni JM. Lipid-lowering, hepatoprotective, and atheroprotective effects of the mixture Hong-Qu and gypenosides in hyperlipidemia with NAFLD rats. J Chin Med Assoc 2016;79:111-21.
PUBMED | CROSSREF

22. Wang M, Wang F, Wang Y, Ma X, Zhao M, Zhao C. Metabonomics study of the therapeutic mechanism of *Gynostemma pentaphyllum* and atorvastatin for hyperlipidemia in rats. PLoS One 2013;8:e78731.
    PUBMED | CROSSREF

23. Müller C, Gardemann A, Keilhoff G, Peter D, Wiswedel I, Schild L. Prevention of free fatty acid-induced lipid accumulation, oxidative stress, and cell death in primary hepatocyte cultures by a *Gynostemma pentaphyllum* extract. Phytomedicine 2012;19:395-401.
    PUBMED | CROSSREF

24. Quan Y, Qian MZ. Effect and mechanism of gypenoside on the inflammatory molecular expression in high-fat induced atherosclerosis rats. Zhongguo Zhong Xi Yi Jie He Za Zhi 2010;30:403-6.
    PUBMED

25. Cai H, Liang Q, Ge G. Gypenoside attenuates β amyloid-induced inflammation in N9 microglial cells via SOCS1 signaling. Neural Plast 2016;2016:6362707.
    PUBMED | CROSSREF

26. Liou CJ, Huang WC, Kuo ML, Yang RC, Shen JJ. Long-term oral administration of *Gynostemma pentaphyllum* extract attenuates airway inflammation and Th2 cell activities in ovalbumin-sensitized mice. Food Chem Toxicol 2010;48:2592-8.
    PUBMED | CROSSREF

27. Willems ME, Myers SD, Gault ML, Cook MD. Beneficial physiological effects with blackcurrant intake in endurance athletes. Int J Sport Nutr Exerc Metab 2015;25:367-74.
    PUBMED | CROSSREF

28. Wang J, Yang JL, Zhou PP, Meng XH, Shi YP. Further new gypenosides from Jiaogulan (*Gynostemma pentaphyllum*). J Agric Food Chem 2017;65:5926-34.
    PUBMED | CROSSREF

29. Lin CC, Huang PC, Lin JM. Antioxidant and hepatoprotective effects of *Anoectochilus formosanus* and *Gynostemma pentaphyllum*. Am J Chin Med 2000;28:87-96.
    PUBMED | CROSSREF

30. Liu J, Zhang L, Ren Y, Gao Y, Kang L, Qiao Q. Anticancer and immunoregulatory activity of *Gynostemma pentaphyllum* polysaccharides in H22 tumor-bearing mice. Int J Biol Macromol 2014;69:1-4.
    PUBMED | CROSSREF

31. Gao D, Zhao M, Qi X, Liu Y, Li N, Liu Z, Bian Y. Hypoglycemic effect of *Gynostemma pentaphyllum* saponins by enhancing the Nrf2 signaling pathway in STZ-inducing diabetic rats. Arch Pharm Res 2016;39:221-30.
    PUBMED | CROSSREF

32. Ding YJ, Tang KJ, Li FL, Hu QL. Effects of gypenosides from *Gynostemma pentaphyllum* supplementation on exercise-induced fatigue in mice. Afr J Agric Res 2010;5:707-11.

33. Wang H, Li C, Wu X, Lou X. Effects of *Gynostemma pentaphyllum* (Thunb.) Makino polysaccharides supplementation on exercise tolerance and oxidative stress induced by exhaustive exercise in rats. Afr J Agric Res 2012;7:2632-8.

34. Kim YH, Kim SM, Lee JK, Jo SK, Kim HJ, Cha KM, Lim CY, Moon JM, Kim TY, Kim EJ. Efficacy of *Gynostemma pentaphyllum* extract in anti-obesity therapy. Rec Nat Prod 2020;14:116-28.
    CROSSREF

35. Yoon J, Ham H, Sung J, Kim Y, Choi Y, Lee JS, Jeong HS, Lee J, Kim D. Black rice extract protected HepG2 cells from oxidative stress-induced cell death via ERK1/2 and Akt activation. Nutr Res Pract 2014;8:125-31.
    PUBMED | CROSSREF

36. Summermatter S, Santos G, Pérez-Schindler J, Handschin C. Skeletal muscle PGC-1α controls whole-body lactate homeostasis through estrogen-related receptor α-dependent activation of LDH B and repression of LDH A. Proc Natl Acad Sci U S A 2013;110:8738-43.
    PUBMED | CROSSREF

37. Sozen B, Ozturk S, Yaba A, Demir N. The p38 MAPK signalling pathway is required for glucose metabolism, lineage specification and embryo survival during mouse preimplantation development. Mech Dev 2015;138:375-98.
    PUBMED | CROSSREF

38. Wright DC, Geiger PC, Han DH, Jones TE, Holloszy JO. Calcium induces increases in peroxisome proliferator-activated receptor γ coactivator-1α and mitochondrial biogenesis by a pathway leading to p38 mitogen-activated protein kinase activation. J Biol Chem 2007;282:18793-9.
    PUBMED | CROSSREF

39. Gerhart-Hines Z, Rodgers JT, Bare O, Lerin C, Kim SH, Mostoslavsky R, Alt FW, Wu Z, Puigserver P. Metabolic control of muscle mitochondrial function and fatty acid oxidation through SIRT1/PGC-1α. EMBO J 2007;26:1913-23.
    PUBMED | CROSSREF

40. Rodgers JT, Lerin C, Gerhart-Hines Z, Puigserver P. Metabolic adaptations through the PGC-1 α and SIRT1 pathways. FEBS Lett 2008;582:46-53.
PUBMED | CROSSREF

41. Ishii T, Itoh K, Takahashi S, Sato H, Yanagawa T, Katoh Y, Bannai S, Yamamoto M. Transcription factor Nrf2 coordinately regulates a group of oxidative stress-inducible genes in macrophages. J Biol Chem 2000;275:16023-9.
PUBMED | CROSSREF

42. Pi J, Bai Y, Reece JM, Williams J, Liu D, Freeman ML, Fahl WE, Shugar D, Liu J, Qu W, et al. Molecular mechanism of human Nrf2 activation and degradation: role of sequential phosphorylation by protein kinase CK2. Free Radic Biol Med 2007;42:1797-806.
PUBMED | CROSSREF

43. Apopa PL, He X, Ma Q. Phosphorylation of Nrf2 in the transcription activation domain by casein kinase 2 (CK2) is critical for the nuclear translocation and transcription activation function of Nrf2 in IMR-32 neuroblastoma cells. J Biochem Mol Toxicol 2008;22:63-76.
PUBMED | CROSSREF

44. Norberg A, Hoa NK, Liepinsh E, Van Phan D, Thuan ND, Jörnvall H, Sillard R, Ostenson CG. A novel insulin-releasing substance, phanoside, from the plant *Gynostemma pentaphyllum*. J Biol Chem 2004;279:41361-7.
PUBMED | CROSSREF

45. Zhang GL, Deng JP, Wang BH, Zhao ZW, Li J, Gao L, Liu BL, Xong JR, Guo XD, Yan ZQ, et al. Gypenosides improve cognitive impairment induced by chronic cerebral hypoperfusion in rats by suppressing oxidative stress and astrocytic activation. Behav Pharmacol 2011;22:633-44.
PUBMED | CROSSREF

46. Yeo J, Kang YJ, Jeon SM, Jung UJ, Lee MK, Song H, Choi MS. Potential hypoglycemic effect of an ethanol extract of *Gynostemma pentaphyllum* in C57BL/KsJ-db/db mice. J Med Food 2008;11:709-16.
PUBMED | CROSSREF

47. Lu KW, Ma YS, Yu FS, Huang YP, Chu YL, Wu RS, Liao CL, Chueh FS, Chung JG. Gypenosides induce cell death and alter gene expression in human oral cancer HSC-3 cells. Exp Ther Med 2017;14:2469-76.
PUBMED | CROSSREF

48. Ahmed I, Leach DN, Wohlmuth H, De Voss JJ, Blanchfield JT. Caco-2 cell permeability of flavonoids and saponins from *Gynostemma pentaphyllum*: the immotal herb. ACS Omega 2020;5:21561-9.
PUBMED | CROSSREF

49. Zhang L, Gong H, Sun Q, Zhao R, Jia Y. Spermidine-activated satellite cells are associated with hypoacetylation in ACVR2B and Smad3 binding to myogenic genes in mice. J Agric Food Chem 2018;66:540-50.
PUBMED | CROSSREF

50. Ambrosio F, Kadi F, Lexell J, Fitzgerald GK, Boninger ML, Huard J. The effect of muscle loading on skeletal muscle regenerative potential: an update of current research findings relating to aging and neuromuscular pathology. Am J Phys Med Rehabil 2009;88:145-55.
PUBMED | CROSSREF

51. Motohashi N, Asakura A. Molecular regulation of muscle satellite cell self-renewal. J Stem Cell Res Ther 2012;Suppl 11:e002.
PUBMED | CROSSREF

52. Takeda K, Machida M, Kohara A, Omi N, Takemasa T. Effects of citrulline supplementation on fatigue and exercise performance in mice. J Nutr Sci Vitaminol (Tokyo) 2011;57:246-50.
PUBMED | CROSSREF

53. Schreiber SN, Emter R, Hock MB, Knutti D, Cardenas J, Podvinec M, Oakeley EJ, Kralli A. The estrogen-related receptor α (ERRα) functions in PPARγ coactivator 1α (PGC-1α)-induced mitochondrial biogenesis. Proc Natl Acad Sci U S A 2004;101:6472-7.
PUBMED | CROSSREF

54. Kang C, Li Ji L. Role of PGC-1α signaling in skeletal muscle health and disease. Ann N Y Acad Sci 2012;1271:110-7.
PUBMED | CROSSREF

55. Boström P, Wu J, Jedrychowski MP, Korde A, Ye L, Lo JC, Rasbach KA, Boström EA, Choi JH, Long JZ, et al. A PGC1-α-dependent myokine that drives brown-fat-like development of white fat and thermogenesis. Nature 2012;481:463-8.
PUBMED | CROSSREF

56. Hosseini Farahabadi SS, Ghaedi K, Ghazvini Zadegan F, Karbalaie K, Rabiee F, Nematollahi M, Baharvand H, Nasr-Esfahani MH. ERK1/2 is a key regulator of Fndc5 and PGC1α expression during neural differentiation of mESCs. Neuroscience 2015;297:252-61.
PUBMED | CROSSREF

57. Chen SQ, Ding LN, Zeng NX, Liu HM, Zheng SH, Xu JW, Li RM. Icariin induces irisin/FNDC5 expression in C2C12 cells via the AMPK pathway. Biomed Pharmacother 2019;115:108930.
PUBMED | CROSSREF

58. Liu J, Li Y, Yang P, Wan J, Chang Q, Wang TTY, Lu W, Zhang Y, Wang Q, Yu LL. Gypenosides reduced the risk of overweight and insulin resistance in C57BL/6J mice through modulating adipose thermogenesis and gut microbiota. J Agric Food Chem 2017;65:9237-46.
PUBMED | CROSSREF

59. Hunter RW, Treebak JT, Wojtaszewski JF, Sakamoto K. Molecular mechanism by which AMP-activated protein kinase activation promotes glycogen accumulation in muscle. Diabetes 2011;60:766-74.
PUBMED | CROSSREF

60. Janzen NR, Whitfield J, Hoffman NJ. Interactive roles for AMPK and glycogen from cellular energy sensing to exercise metabolism. Int J Mol Sci 2018;19:3344.
PUBMED | CROSSREF

61. Ha J, Guan KL, Kim J. AMPK and autophagy in glucose/glycogen metabolism. Mol Aspects Med 2015;46:46-62.
PUBMED | CROSSREF

62. Hingst JR, Bruhn L, Hansen MB, Rosschou MF, Birk JB, Fentz J, Foretz M, Viollet B, Sakamoto K, Færgeman NJ, et al. Exercise-induced molecular mechanisms promoting glycogen supercompensation in human skeletal muscle. Mol Metab 2018;16:24-34.
PUBMED | CROSSREF

63. Ehrenborg E, Krook A. Regulation of skeletal muscle physiology and metabolism by peroxisome proliferator-activated receptor delta. Pharmacol Rev 2009;61:373-93.
PUBMED | CROSSREF

64. Scarpulla RC. Transcriptional paradigms in mammalian mitochondrial biogenesis and function. Physiol Rev 2008;88:611-38.
PUBMED | CROSSREF

65. Hayes JD, Dinkova-Kostova AT. The Nrf2 regulatory network provides an interface between redox and intermediary metabolism. Trends Biochem Sci 2014;39:199-218.
PUBMED | CROSSREF

66. Demine S, Renard P, Arnould T. Mitochondrial uncoupling: a key controller of biological processes in physiology and diseases. Cells 2019;8:795.
PUBMED | CROSSREF